Astron. Astrophys. 332, 93–101 (1998)

ASTRONOMY
AND
ASTROPHYSICS

HST/WFPC2 observation of the core of M 3: Blue objects and the position of the radio source

M. Laget[1], **F.R. Ferraro**[2], **B. Paltrinieri**[2], **and F. Fusi Pecci**[2,3]

[1] Laboratoire d'Astronomie Spatiale du CNRS, B.P. 8, F-13376 Marseille cedex 12, France (laget@astrsp-mrs.fr)
[2] Osservatorio Astronomico di Bologna, Via Zamboni 33, I-40126 Bologna, Italy (Ferraro, L_Paltrinier, Flavio@astbo3.bo.astro.it)
[3] Stazione Astronomica, I-09012 Capoterra, Cagliari, Italy

Received 23 September 1997 / Accepted 5 December 1997

Abstract. HST/WFPC2 images of the central part of the globular cluster M 3 (NGC 5272) in UV (F255W), U (F336W), V (F555W) and I (F814W) are used to search for faint blue stars down to an UV magnitude slightly below the turnoff level. Three low-luminosity blue stars are found in the PC1 field of view; two are new detections. All are within $\sim 10''$ from the cluster centre. Two are likely horizontal branch stars on the extreme blue extension which turns out very scarce in the core of this cluster. The third object has a position in the UV color-magnitude diagram consistent with the cataclysmic variables region; changes in its magnitude during the limited period of observation provide marginal indication of variability. One of the very few known non-pulsating radio sources, located in the direction of the centre, is accurately positioned. Its position does not match any of the low luminosity blue stars by $\sim 7''$. In turn, the error box of the radio source position contains two interesting objects: a bright horizontal branch star and a bright blue straggler, both are within $\sim 1''$. No other object in the vicinity of the radio source shows any photometric signature of an unusual cluster object or of an extragalactic source. Variability of some candidates (RR Lyrae and BSS) has been confirmed; new variable candidates of both types have also been found.

Key words: globular clusters: individual: M 3 – globular clusters: general – stars: population II – ultraviolet: stars – radio continuum: stars

1. Introduction

Globular cluster cores are now known to harbor -if not produce- a variety of exotic objects. Extreme horizontal branch stars (Brown et al. 1997; Dorman et al. 1993), blue straggler stars (Bailyn 1995), low mass X-ray binaries (Parmar 1992), cataclysmic variables (Grindlay 1992; Bailyn et al. 1990), millisecond pulsars (Lyne 1995) or binaries (Hut et al. 1992) are *test* objects whose presence brings clues to important aspects of stellar evolution. Their nature, number and radial distribution provide also insights on the combined influences of dynamics and star density on the evolution of a coeval, simple stellar population (Fusi Pecci et al. 1993; Djorgovski et al. 1991). Most are variable or suspected variable and have a signature in the ultraviolet. These objects are actively searched in cluster cores and in their outskirts.

The bright galactic globular cluster M 3 (NGC 5272) is a typical benchmark for this type of studies. It has an intermediate metallicity and concentration, and it displays a well populated horizontal-branch (HB), extending from the red to the blue side of the instability strip, but with a very sparse blue extension (Sandage 1953, Buonanno et al. 1994). M3 has a large population of blue straggler stars (BSS) (Ferraro et al. 1993; Bolte et al. 1993; Burgarella et al. 1995; Guhathakurta et al. 1994) with a very unusual bimodal radial distribution (Ferraro et al. 1997a) which suggests either different formation mechanisms or, more specifically, that special destruction/survival and segregation effects have taken place in the core of this cluster. An unsuccessful search for cataclysmic variables down to $M_{\rm B} < 6$ was also reported by Shara et al. (1985).

In addition, and most relevant, deep radio synthesis images have provided evidence for a non-pulsating, point radio source in the direction of the very cluster centre, possibly related to a pulsar in a very compact binary system or to an unrelated background object (Kulkarni et al. 1990). To our knowledge, the source has not been identified at optical wavelengths. Two radio sources located in the cluster outskirts ($5 < r < 10'$), tentatively identified as cluster stars at a modest radio resolution (Klemola 1979), are now thought to be associated with background QSO's (Carney 1976; Harris et al. 1992) as probably is an other nearby radio source M 3A (McLean et al. 1983). The fact that a typical low-redshift QSO would also appear as a blue object emphasizes the need for a search for faint blue objects within the cluster core and for a precise positioning of the radio source at optical wavelengths.

Send offprint requests to: M. Laget

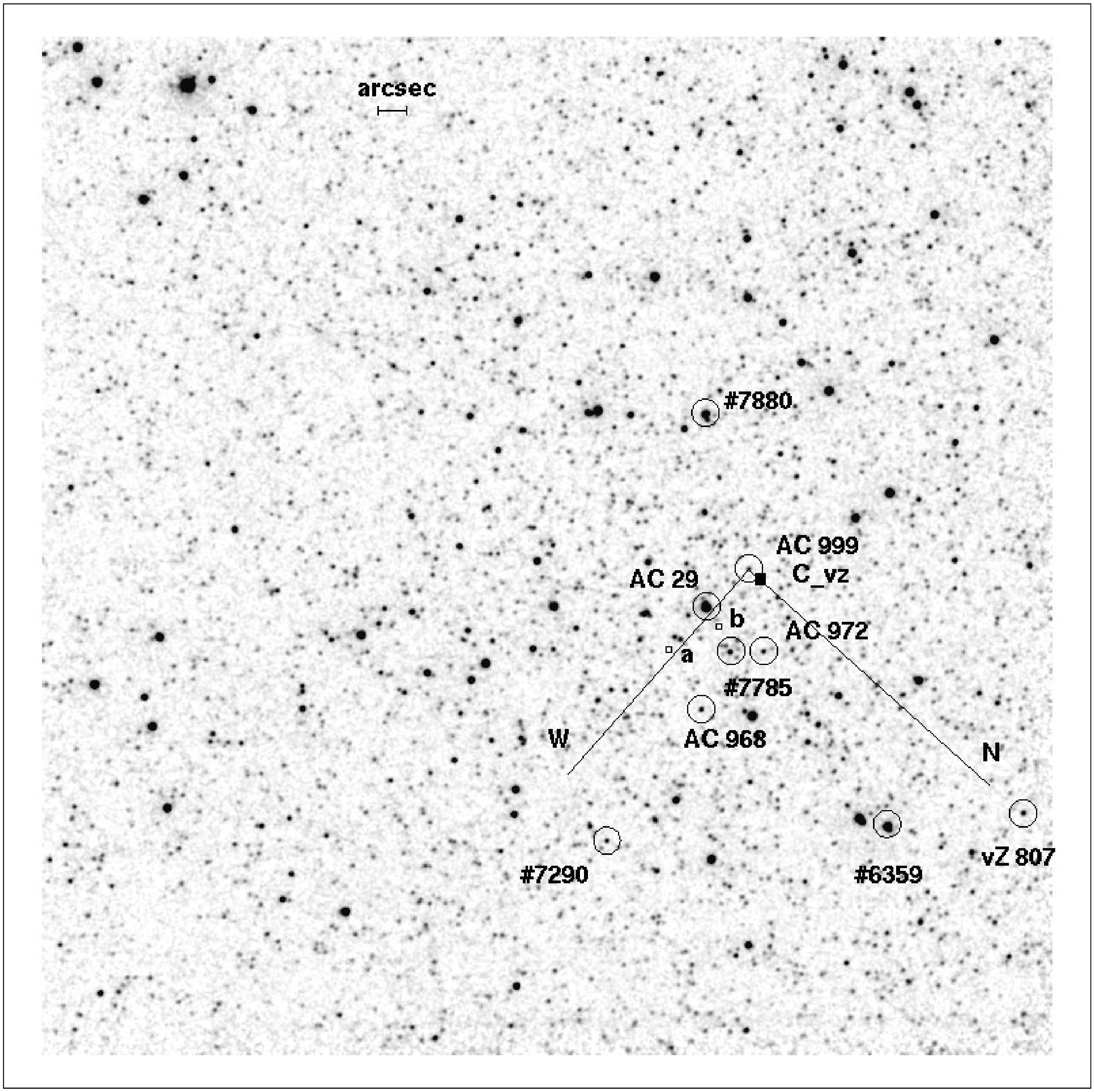

Fig. 1. The ultraviolet (F255W) image of the core of M 3 obtained with the HST/WFPC2 PC1 camera is displayed. The image is the median of four 300 sec exposures. For the sake of visualization, a filtering by a gaussian (3x3 pix., σ = .5 pix.) has been applied. The intensity scale is linear. Reference stars are labelled as AC (from Aurière & Cordoni, 1983). AC29 (#7521) is a bright horizontal branch star, #7785 is a blue straggler. Small open squares labelled "a" or "b" refer to the expected positions of the radio source discussed below. The cluster centre as defined by von Zeipel (1908) (labelled C_vz; filled square) is at $\sim 0.05''$ East and $\sim 0.43''$ north of star AC999. The orientation and the approximate plate scale are indicated.

In this paper we report a search for faint blue objects in the core of M 3 carried out using HST/WFPC2 images aimed, in particular, at the detection of any possible candidate counterparts for the known central radio source.

2. Observations and data reduction

The central region of M 3 was observed with the WFPC2 on 25 April 1995 (GO-proposal #5496; P.I: FFP). The cluster core was imaged on the 35″ field of view of the PC1 which has a linear scale of 0.04554″ per pixel. Four sets of exposures of 300, 800, 100 and 140 sec were sequentially taken in U (F336W), V (F555W), I (F814W) and UV (F255W) respectively. Exposures were performed between the date 1995.115:10:17:39 and 1995.115:16:50:39. Here we discuss essentially the PC1 images which properly sampled the cluster core.

The raw data images were first processed by the standard HST/WFPC2 procedure as far as the data handling, flat-fielding and pixel corrections are concerned. For every filter, the images were median filtered to remove the cosmic rays, and the resulting image has been used to search for all the objects present in each field. The PSF fitting photometry was then performed on each individual frame separately using the HST-updated version of ROMAFOT (Buonanno et al. 1979, 1983). The complete description of the available material, the reductions, and other results will be presented elsewhere (Ferraro et al. 1997b and in preparation). The instrumental magnitudes have been transformed into the UVI-Johnson system following the prescription given by Holtzman et al. (1995); the F255W magnitudes are in the STMAG system. To avoid low count statistics we have set a limiting magnitude cut-off at U = 20.5 beyond which the photometry becomes less reliable and we only consider hereafter objects which fulfilled the following requirements:

i)- the star image in the F255W filter consists of, at least, two pixels at 5σ ($\sim$ 1.6 DN) above the sky background;

ii)- the star image is present on all four images taken with the same frame. The individual images of the stars of interest were manually checked for the occurrence of multi-pixel cosmic rays events;

iii)- the candidate star has detectable counterparts at all wavelengths (2550, 3360, 5550 and 8140Å);

Stars located within 2 arcsec from the frame edges were rejected as well as those heavily affected by known hot pixels or bad columns. Fig. 1 displays the image of the cluster core through the F255W filter.

3. The observational data

3.1. The UV color excess: detection and photometry of three objects

The images in the filters F255W and F336W (U) were used to construct the UV-CMD ($m_{255} - U, m_{255}$) which is the most suitable diagram to detect UV-bright sources in a background dominated by cool stars. Fig. 2 displays the ultraviolet CMD of the very central region of the cluster, based on the PC1 data set only.

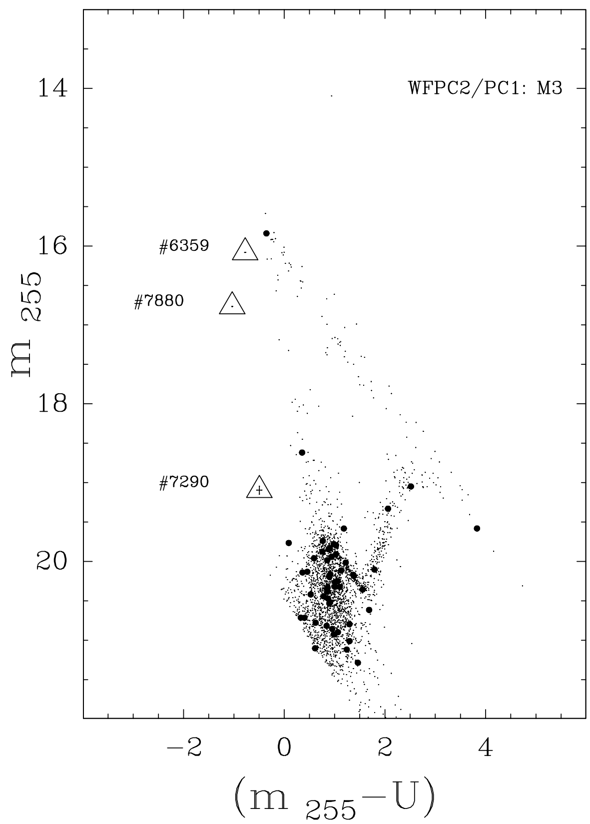

Fig. 2. ($m_{255} - U, m_{255}$) UV-CMD for 3063 stars identified in the PC1 field of view. The outliers #6359, #7880 and #7290 are shown with their errors. Stars found within the error box of the expected position of the radio source (see Sect. 4) are plotted as filled circles. The lower left cut-off corresponds to U = 20.5.

The most striking feature in the UV-CMD is the locus defined by the "horizontal branch", which runs across the diagram and ends sharply with no extension at higher temperatures and lower luminosities but a few objects. The second remarkable feature is the sequence of blue straggler stars which has been analysed in Ferraro et al. (1997a). The bright, UV-bright candidate Post-AGB star at $\sim$ (1.0,14.0), will be discussed in a forthcoming paper (Ferraro et al. 1997b). The CMD is expected to be substantially complete to $m_{255} \sim 20$.

Three objects (#6359, #7880 and #7290) appear bluer than ($m_{255} - U$) = −0.5 and lie significantly outside the main locus of cluster stars in the UV-CMD. They are plotted as empty triangles in Fig. 2. They are well above the 5σ limit from the sky background, and the formal errors computed for all three stars (illustrated in the same diagram) show that their color is reliable. Their detection in every frame and at every wavelength indicates that they are real features. Their position is circled and labelled in Fig. 1.

The relatively bright star #6359 has a counterpart #1105 (V = 17.58 $V - I$ = −0.05) in the catalogue of the pre-refurbishment WF-PC1 data of Guhathakurta et al. (1994, Tables 2 and 3; hereafter GYBS). The two faintest stars are new detections since they are listed neither in GYBS nor in the deep

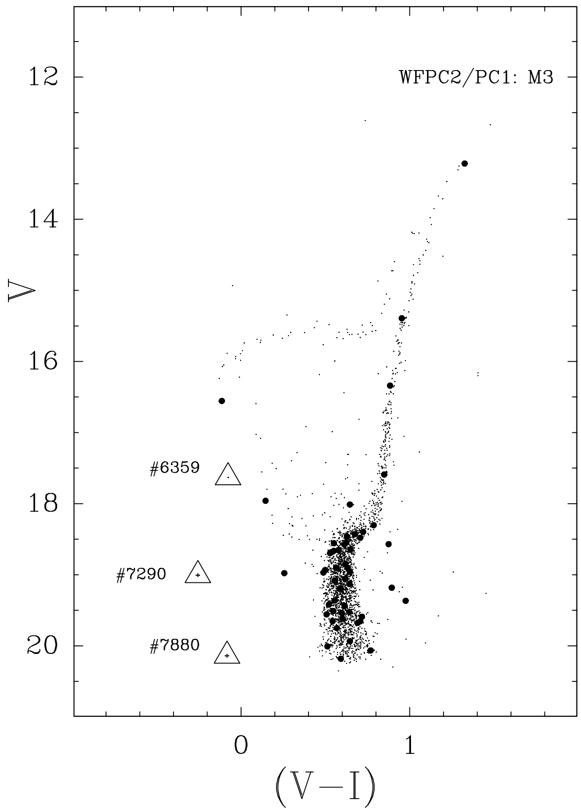

Fig. 3. $(V-I, V)$ CMD for stars shown in Fig. 2. The positions of the three stars discussed here (namely #6359, #7880 and #7290) are shown. Symbols are the same as in Fig. 2.

Table 1. V, I, U, m_{255} magnitudes for the three faint blue objects shown in Figs. 1 and 2. Stars #7284 and #7879 are close neighbours of #7290 and #7880, respectively.

Id	V	I	U	m_{255}
7290	20.15	20.23	19.60	19.10
7880	19.01	19.27	17.81	16.77
6359	17.63	17.71	16.86	16.08
–	–	–	–	–
7284	20.20	19.22	20.41	–
7879	18.32	17.93	18.55	19.10

ground-based catalogue of Ferraro et al. (1997e). The stars of Fig. 2 are also plotted (Fig. 3) in the $(V-I, V)$ CMD to allow an easier comparison with HST or ground-based CMDs of M 3 as well as with the CMD's of other clusters.

Though in this paper we limit the discussion to the PC1 data, the same procedure to select candidate blue objects has already been applied to the WF2, WF3 and WF4 fields. All preselected UV-bright, low luminosity candidates turned out to be either spurious events (mainly cosmic rays) or too faint to be statistically reliable and they did not survive the specific requirements listed in Sect. 2. Therefore, within the completeness, the low luminosity blue stars are also very rare in the three surrounding chips covering about 12 times the PC1 area. This conclusion is also strengthened by a simple simulation showing that in the WF's (which have half the PC1 angular resolution) any star like the faintest blue PC1 stars #7290 and #7880, which both have a very close neighbour red main sequence star, would have merged into composite systems that would still have been selected as photometrically peculiar in the UV-CMD.

The already noted scarcity of such stars in the ground-based CMD (Buonanno et al. 1994) obtained in the external regions is also confirmed here for the cluster central region. In this respect, M 3 is remarkably different from M13, a very similar cluster with the same metal abundance which exhibits a very populated blue HB extension in its core (Ferraro et al. 1997c) and in the outer regions (Paltrinieri et al. 1998).

3.2. First hints on their nature

In the previous section we have found that there are very few faint blue objects in the cluster core of M 3 and that they are all confined within $10''$ from the cluster centre ($\sim 0.4 r_c$). This peculiar location strongly suggests that they are cluster members, though background extragalactic sources or foreground stars cannot be a priori excluded.

Background sources can be quasars as inferred from the spectral identifications of optical counterparts of radio sources at 20 cm (Harris et al. 1992; Carney 1976) within $\sim 5'$ from the centre. The fact that there is no spectral information on the radio source in M 3 (which in addition does not show any pulsation, Kulkarni 1997, private communication) makes difficult to exclude that the source is a quasar. To further investigate this possibility in Fig. 4 we compare the colors of the blue sources identified here with the colors expected for a redshifted quasar computed by folding a representative composite spectrum in the 900-8000 Å range (Cristiani & Vio, 1990) with the PC1 filters (including red leaks). Although the colors of a QSO may deviate from that of the composite spectrum used here, the three objects cited above do not occupy the region of the color-color diagram representative of a low redshift QSO. Though not plotted here for clarity, none of the 3064 PC1 field objects which have a UV magnitude occupy the quasar region neither, suggesting that if the radio source is actually a low redshift quasar, the presently undetected optical counterpart is likely fainter than $B \sim 21.5$ ($m_{255\,\mathrm{lim}} \sim 20.5$). The apparent lack of objects with colors consistent with those of a quasar all over the PC1 field, probably rules out also the possibility of a point-like complex radio structure associated to an optical counterpart but with a significant ($> 10''$) offset, as illustrated for quasars of the cluster outskirts (Harris et al. 1992).

In Fig. 4 the three objects (which in the following we will consider as stars -either single or multiple) are located above the main sequence locus which is derived from integration of the models of stellar atmospheres (Kurucz 1992) in the WFPC2 filters bands. The models are for main-sequence stars (log g = 4.0) and for a normalized logarithmic metal abundance relative to the sun of -1.5. The curve was slightly translated along the $m_{255} - V$

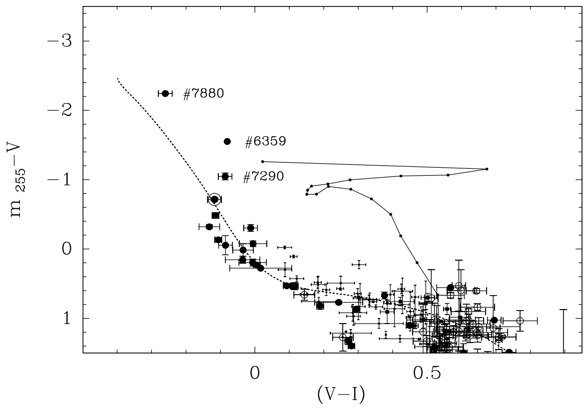

Fig. 4. Colour-colour Diagram for the bluest stars found in the PC1 field of view: HB stars have been plotted as filled circles, BSS as dots, yellow stragglers as filled square, respectively. The three blue objects discussed in the text are labelled. The Kurucz's models for main sequence stars at $logA = -1.5$ are plotted as a dashed line. Connected dots indicate the colors of a representative quasar per 0.1 step in redshift; the dramatic change in the $V-I$ color traces H_α in the triangle shaped I filter. As can be seen the three blue objects have bluer colours with respect to typical QSOs. AC29 (#7251) is circled. Open circle, are all the objects lying within 3σ error box ($\pm 3.8''$, $\pm 1''$) from the radio source position; none has a remarkable blue color.

color, to fit the region of the low luminosity, presumably unevolved blue stragglers. All the three stars occupy the typical UV excess region of faint blue stars.

The local space densities ($7\times10^{-7}, 2\times10^{-6}$ and 7×10^{-4}) pc^{-3} measured by Downes (1986) for the most abundant field faint blue stars namely, O-, B-type subdwarfs and hot white dwarfs respectively, would lead to less than 10^{-3} hot white dwarf in the $35''$ PC1 field of view, within the volume of space defined by twice the scale height of 325 pc (90% of the population) derived by Green et al. (1986). The negligible contributions expected from any stellar species of the field, coupled with the evidence that the stars are towards the very cluster centre, indicate that they are probable cluster members. Table 1 summarizes the photometry for all these stars.

The two brightest UV stars (#6359 and #7880) appear to lie on the extension of the HB which is better visible in Fig. 2 of Ferraro et al. (1997c) in which the ($m_{255} - U, m_{255}$) CMD of M 3 is compared with that of M13, obtained with the same set-up. Once the CMD of M 3 is shifted to match the main loci in the M13 one, these two stars perfectly merge into the M13 HB blue tail. For this reason they are very likely *normal* HB stars, with a very thin residual hydrogen envelope (Dorman et al. 1993). Since they are only found so close to the cluster centre, one could speculate that star interactions occurring within the very inner region of the clusters could be somehow related to the origin of the HB blue tail population (Fusi Pecci et al. 1993), at least in some clusters as discussed in Ferraro et al. (1997c).

The object #7290 is located outside the main loci and shows a substantial UV excess. Its position is similar to the two faint UV-stars recently discovered in the core of M 13 (Ferraro et al. 1997d), which have been found to be possibly connected to the X-ray source detected in that cluster. In fact, star #7290, though slightly cooler ($\delta(m_{255} - U) \sim 0.8$), has nearly the same UV absolute magnitude ($M_{255} \sim -4.1$) than the brightest UV-star in M13. Assuming a distance modulus of 15.08 (Webbink, 1985), #7290 would have an absolute visual magnitude of ~ 5.1, consistent with the observed range ($4 < M_V < 11$) for the cataclysmic variables (Warner, 1987). This star deserves a more detailed follow-up study.

4. Positioning the radio source within the centre of M 3

Within the precise VLA coordinates system, the position of the radio source (Kulkarni et al. 1990) is:

$$\text{R.A.}_{\text{RS}}(1950) = 13^h39^m53^s.14$$

$$\text{DEC.}_{\text{RS}}(1950) = 28°37'44''.72$$

with a quoted error of $\sigma \sim 0.15''$ (on each axis).

At optical wavelengths, in the von Zeipel (1908) reference frame, the coordinates of AC999 (a bright star close to the adopted cluster centre) can be derived from Aurière and Cordoni (1983):

$$\text{R.A.}_{\text{AC999}}(1950) = 13^h39^m53^s.49$$

$$\text{DEC.}_{\text{AC999}}(1950) = 28°37'44''.57$$

.

The relative position of the radio source with respect to AC999 (labelled "a" in Fig. 1) is then derived at:

$$\Delta\text{R.A.}_{\text{RS}-\text{AC999}} = -4.69''$$

$$\Delta\text{DEC.}_{\text{RS}-\text{AC999}} = -0.17''$$

However, Aurière & Cordoni (1983) have pointed out that the coordinates system adopted by von Zeipel (1908) differs by a few arcsec from that of Sawyer Hogg (1973). Gunn & Griffin (1979) have also noticed that for the star vZ807, the system used by von Zeipel differs from that of Barnard (1931) by 1.8 and 0.2 $''$ in R.A. and DEC. respectively, suggesting that the Right Ascension derived in the von Zeipel reference may be uncertain by an appreciable amount.

None of the recent reference catalogues of positions like the Automatic Plate Measuring System (APM) of the Institute of Astronomy at Cambridge or the Positions and Proper Motions catalogues (PPM1) (Roeser & Bastian, 1988) has any star within the field of the PC1 on which we can rely to set up a new safe coordinates system. The nearest PPM star is actually at $7.3'$ from the centre and no star closer than $\sim 2'$ from the cluster centre has been measured in the APM.

Using a different approach, we made an independent redetermination of the coordinates of AC999 in the APM system. To do this, we used the catalogues of stars measured in M 3 with known counterparts in the APM. First, the ground-based photometric catalogue of the central part of M 3 (Ferraro et al. 1997e) and the photometric catalogue of Buonanno et al. (1994) of the cluster outskirts were merged into one single catalogue. Besides magnitudes and colors, the two catalogues provide also the relative positions of stars with respect to a common origin within better than one tenth of an arcsec (the origin does not actually correspond to any star but falls in the immediate vicinity, $\sim 3''$ north of AC972). The merged catalogue lists the star AC999 and extends sufficiently far from the central part ($7'$) to include a significant number of APM stars. For 309 matched stars, the relative positions of the merged catalogue were directly listed with their corresponding APM coordinates. The coordinates of the common origin were then re-determined as a free parameter from the set of equations, in the APM system of coordinates. The resulting gaussian distributions of the coordinates for the origin have the following mean values:

$$\text{R.A.} = 13^{\text{h}}39^{\text{m}}53^{\text{s}}.20$$
$$\text{DEC.} = +28°37'48''.0$$

with a standard deviation $1.27''$ in R.A. and $.3''$ in DEC. respectively. Since the star AC999 (#10852 in Ferraro et al. 1997e) is $X = 1.3''$ and $Y = -4.0''$, hence the APM (B1950) coordinates of AC999 would be:

$$\text{R.A.} = 13^{\text{h}}39^{\text{m}}53^{\text{s}}.299$$
$$\text{DEC.} = +28°37'44''.0$$

and the difference between the radio source and AC999 would be:

$$\Delta\text{R.A.}_{\ \text{RS}-\text{AC999}} = -2.09''$$
$$\Delta\text{DEC.}_{\ \text{RS}-\text{AC999}} = +0.72''$$

the corresponding position is labelled "b" in Fig. 1 and in Fig. 5.

The APM plates (Irwin & Trimble 1984) were originally aligned with respect to PPM astrometric standards. In the region of M 3, for 11 APM stars which have their counterpart in the PPM1, we have measured a mean difference of:

$$\Delta\text{R.A.}_{\ (\text{PPM1}-\text{APM})} = 0.6'' \pm 0.8$$
$$\Delta\text{DEC.}_{\ (\text{PPM1}-\text{APM})} = -0.14'' \pm 0.6$$

Although the dispersion is large and the number of stars in common is limited, the two catalogues are in reasonable agreement. Hence, the determination of the coordinates of AC999 and the position of the radio source are consistent with the PPM1.

Finally, an additional and independent determination of the location of the radio source within the PC chip was performed by using the IRAF task INVMETRIC which transforms the celestial coordinates into WFPC2 pixel coordinates making allowance of the geometrical distortions. In the HST image, the radio-source ($\text{R.A.}_{2000} = 13^{\text{h}}42^{\text{m}}11^{\text{s}}.4$ $\text{DEC.}_{2000} = +28°22'38''.0$) is positioned at pixel (369, 292), which is nearly coincident with the position found if one uses the APM reference coordinates (position "b" in Fig. 1).

In conclusion, also given this remarkable coincidence we will adopt in the following, position "b" as the most probable location of the radio source in the PC1 frame.

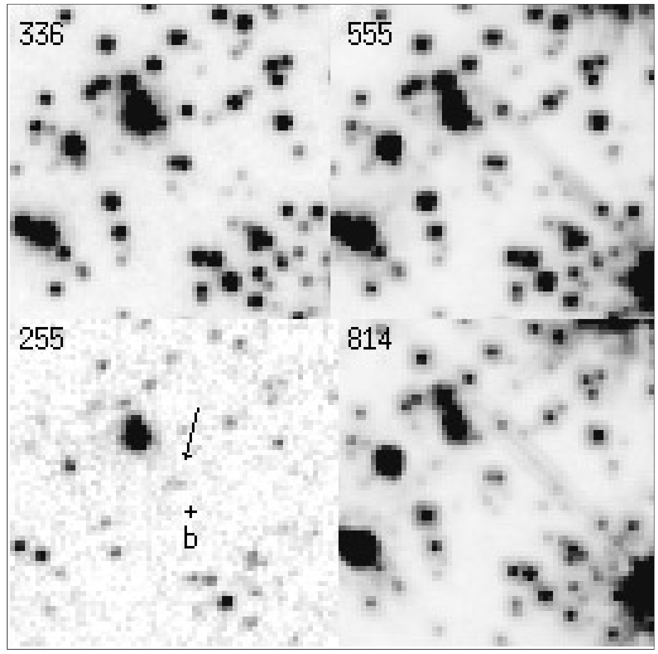

Fig. 5. The enlarged region of the best estimate of the radio source position ("b") is displayed at all wavelengths. The nearest faint feature (arrow) at UV wavelengths is actually a blend of faint regular main sequence stars, best seen in the visible filters; no variability over the period of observation nor an unusual color is found for these two stars.

5. Discussion

From the previous analysis it turns out that the best estimate of the radio source position is almost equally distant from the three faint blue stars we have found in the PC1 field of view. None is closer than $6.8''$ and consequently none is a realistic candidate for the optical counterpart. The nearest detected object is a faint feature in the F255W image (see Fig. 5), clearly visible in the V and I filters as a blend of two main sequence stars.

We have plotted (as filled circles) in the CMD of Fig. 2 and in the color-color diagram of Fig. 4 all the objects found in the error box ($\pm 3.8'' \times \pm 0.9''$; 3σ) centered on the position of the radio source. As it can be observed, they essentially occupy the expected positions for cluster stars, including the two faint main sequence stars found close to the best estimate of the radio source position shown in Fig. 5. However, looking at Fig.1, it is interesting to note that the position of the radio source is nearly at the same distance ($\sim 1''$) from two bright objects which require further comments: the bright HB star #7251 (AC29) and the bright BSS #7785.

•star #7251

This is one of the brightest HB star in the PC chip ($V = 16.56$ and $V - I = -0.12$). A straightforward identification with the catalogue of Aurière & Cordoni (1983) yields coincidence with star AC 29, which is however listed as a red star ($V = 15.24$, $B - V = 0.75$), rather than a blue object as we find here. The same object is also identified with stars #1247 ($V = 16.54$ and $V - I = 0.00$) in the catalogue of GYBS and with #10849 ($V = 16.05$ and

$V-I=0.06$) in Ferraro et al. (1997e). In the UV, U, V and I frames studied here, #7251 has a resolved fainter companion #7262 ($V=17.93, V-I=0.57$) which is located in the faint yellow straggler-subgiant transition region in the UV as well as in the visible CMD's. If we merge the two components, the resulting composite system ($V=16.28, V-I=0.07$) is consistent with the observations of GYBS and Ferraro et al. (1997e) done at lower angular resolutions. However, it would still deviate (by much more than the plausible uncertainty associated to the measures) from the observations carried out in 1978 and reported by Aurière & Cordoni (1983). Variability may be suspected as a possible cause for the large color variation. Alternatively, a different impact of crowding in the different ground-based observations may also change the derived colors.

Once deblended, #7251 is one of the brightest star in UV, while in the visible CMD ($V, V-I$), the star position is more ambiguous as it lies between the tip of the blue straggler sequence and the blue end of the HB. A conclusive explanation of this peculiar location can hardly be drawn at this stage.

•star #7785

This star ($V=17.96, U=18.27, m_{255}=18.62$) is listed as a bright BSS in the global sample of BSS in M 3 presented by Ferraro et al (1997a). It has also been detected by GYBS (#1196 in their catalogue) and similarly classified as BSS. This star is also present in the Bolte et al. (1993) survey, but it was not identified as BSS since it lies in the region between the BSS extension and the RGB. This is however probably due to the much lower resolution of ground-based observations rather than to variability.

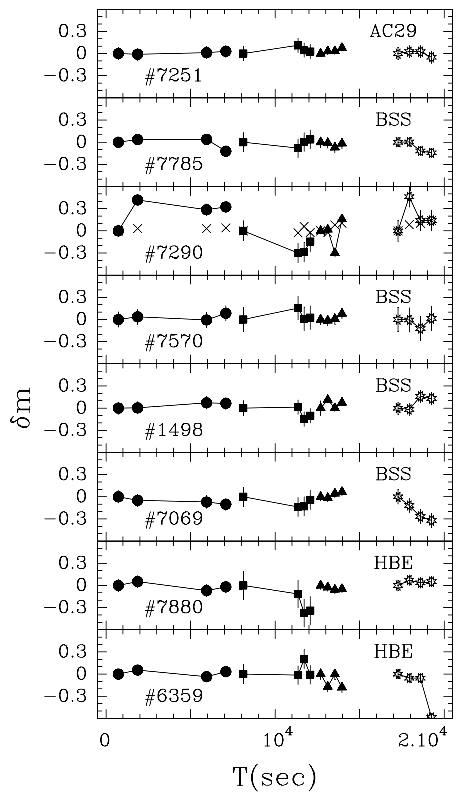

Fig. 6. Composite light curves for possible variable objects. The relative instrumental magnitude variation with respect to the first acquired measure in each filter is plotted as a function of time. The error bars, calculated from the frame-to-frame scatter are also reported. Each filter is coded as follow: filled circles (U), filled squares (V), filled triangles (I) and asterisks (UV), respectively; crosses are for a nearby unblended star, slightly fainter in U,V and I than #7290 and sharing the same sky background. The zero-point reference of the time scale is assumed on 25 April 1995, $UT: 10:00:00$.

5.1. Variability

The search for variables with periods of a fraction of a day and with amplitudes in the range of tenths of a magnitude is commonly used to identify RR Lyrae, cataclysmic variables or contact binaries in cluster cores (Guathakhurta et al. 1994 (M 3); Gilliland et al. 1995, (47 Tuc); Shara et al. 1995; Bailyn et al. 1996, (NGC 6752); Cool et al. 1995 (NGC 6397).

Within the present set of observations, since none of the selected filters is sensitive to the H_α line, we have first searched for a short-term variability of the continuum by monitoring the sequence of measured magnitudes over the observing time for each star of interest. Then, using a different approach, we have also compared the magnitudes listed by two independent catalogues of observations for stars matched by their position.

Short term temporal variability was examined by plotting the residuals of instrumental magnitudes (with respect to the first acquired measure) for each available image in each filter versus time. The composite light curves which are thus derived span more than 5 hours and are displayed in Fig. 6.

Clearly there is no significant variation of the measured magnitudes for the bright HB star #7251 and for the BSS #7785 which are both found near the expected position of the radio source nor for #7880 and #6359 (the two stars lying on the HB extension). The observed changes for star #7290 are more questionable. Variations in U and V with amplitudes $\delta > \pm 0.3$ mag are larger than the internal errors computed from the rms frame-to-frame scatter at the luminosity level of the star. No significant change is observed in I- or in the UV-band respectively. The negligible residual magnitudes observed for a nearby, fainter reference star, sharing the same local background (plotted as crosses in Fig. 6 (#7290)) excludes the local background as a possible source of the observed variations in U and V. We conclude to a marginal evidence of variability for this star.

Variability was also explored by comparing the presently observed UVI magnitudes with those listed in the catalogue of GYBS, based on the pre-refurbishment WFPC1 *HST* images. The two catalogues have a significant overlapping region (40% of the field covered by our PC1). Observations are separated by about three years. A set of 346 stars matched by their position was then extracted and analysed. The faint star #7290 has no counterpart in the GYBS catalogue.

The residuals (WFPC2-WFPC1) in the I,U,V magnitudes respectively, for the 346 stars in common, are plotted in Fig. 7. Nine stars (labelled in the figure) have residuals larger than 3σ in, at least, one filter and are considered as variable candidates.

Table 2. List of the candidate variable stars. Variability in simultaneous bands is noted (UVI). The identification are from Ferraro et al. (1997a - F97) and GYBS.

Id	$Var.$ (UVI)	$Type$ $(F97)$	$Type$ $(GYBS)$	Id $(GYBS)$
1498	UI	BSS	BSS	576
2756	U	–	RRL	684
3465	UVI	–	RRL	507
3472	V	–	RRL	552
5439	I	–	–	864
5923	V	–	RRL	734
7069	V	BSS	BSS	1457
7364	U	–	–	1029
7570	UV	BSS	BSS	1082

They are plotted as full dots in all the panels of Fig. 7 and are listed in Table 2, where the GYBS identification number is also reported. Variability is confirmed for four out of seven RR Lyr as listed by GYBS (see their Table 3) which fall in the common region of observation. The stars #5439 and #7364 are additional candidate variables; their position within the instability gap in the visible CMD is consistent with RR Lyrae type variables. The two stars located near the radio source (#7251, #7785) are both well within the 3σ of the regression line and do not show evidence for variability over the time scale sampled by our observations.

We measure changes in the observed magnitudes (which may indicate variability) for three well established blue straggler stars. BSS #1498 is one of the two blue straggler stars (#576; P< 10 hr) found variable by Guhathakurta et al. (1994) and its variability is confirmed here in U- and in the I-bands. Interestingly, this blue straggler may show out-of-phase variations in the various bands as observed for RR Lyrae-type pulsating stars. #7069 (#1457 in GYBS) is a new candidate BSS variable.

The faint BSS #7570 is listed as a blue straggler in Ferraro et al. (1997a) and in GYBS (#1082), who noted that this candidate blue straggler was not detected by Bolte et al. (1993). While this could be interpreted as a further evidence for a strong variability supported by the present observations, a close look at the WFPC2 images indicates that this star is member of a barely resolved blend, best visible at F336W, with about equal components. It is likely that this blend was not angularly resolved with the unrepaired HST, resulting as a brighter object in the catalogue of GYBS. Hence, the suspected large variability of this blue straggler is probably an artifact.

The composite light curves for the three BSS are also displayed in Fig. 6. The most remarkable feature is the weakening of the UV magnitude of #7069. A trend seems also present in U. This behaviour is not seen in the visible bands. This BSS, like #1498, shows out-of-phase variation in UV and in the visible.

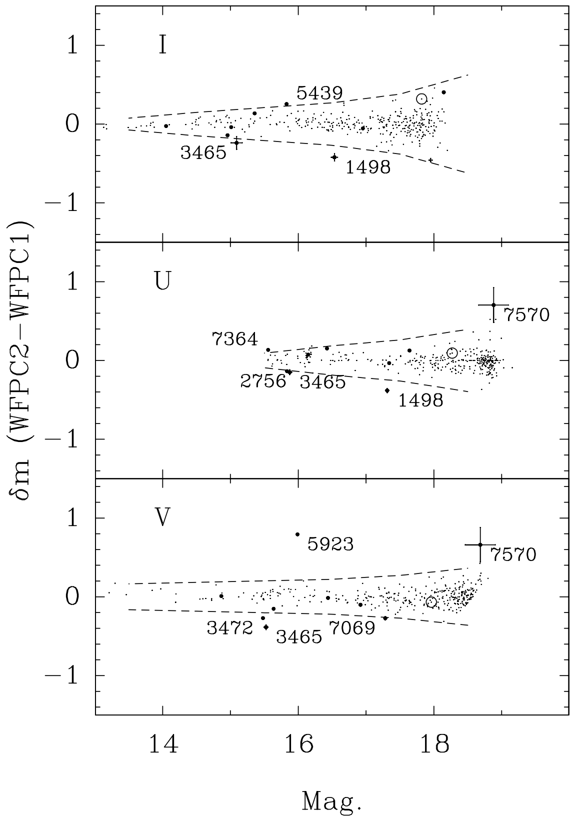

Fig. 7. UVI magnitude residuals between the data presented in this paper (WFPC2) and the pre-refurbishment WFPC1 magnitudes presented by GYBS, for the 346 stars in common, plotted versus our magnitudes. The dashed lines represent the 3σ envelopes. Candidate variables are plotted as heavy dots superimposed to their error bars and they are labelled with their internal running number. Their position is indicated at all wavelengths. Star #1498 is the blue straggler #576 of GYBS: variability is not apparent in V but shows up in U and I. The position of the BSS #7785, close to the radio source position, is circled.

6. Conclusion

HST-WFPC2 images in the ultraviolet (F255W) and in the visible (U, V, I) have been used to search for faint blue stars –down to an ultraviolet magnitude slightly below the turnoff– in the core of the globular cluster M 3.

The paucity of such stars already noted from ground-based observations in the outer regions of this cluster is also confirmed in the very cluster centre. One remarkable feature in this respect is that the only two blue stars lying on the HB extension are confined within $\sim 10''$ from the cluster centre. We were unable to detect any other faint blue star in the three surrounding WF's chips. This could perhaps suggest that they might be somehow the product of dynamical interactions.

Another low luminosity (namely, #7290), possibly variable has been discovered in the very central region of the cluster. The still unidentified, non-pulsating radio source detected in the very centre of M 3 has been precisely positioned and its 3σ error box is not closer than $\sim 5''$ from this peculiar object, too far to be safely identified as its optical counterpart. In turn, the radio source position is close (1″) to an intermediate-temperature HB star (#7251) which might be variable and to a bright BSS (#7785). There are not objects with colors representative of that of a QSO in the PC1 field of view.

Our conclusion is that probably none of the selected objects can be safely identified as the optical counterpart of the radio-source, though a few objects located within the error box deserve dedicated follow-up studies.

Acknowledgements. The financial support by the Agenzia Spaziale Italiana (ASI) is gratefully acknowledged.

References

Aurière M., Cordoni J-P. 1983, A&AS 52, 383
Bailyn C.D., 1995, ARA&A 33, 133
Bailyn C.D., Rubenstein E.P., Slavin S.D. et al., 1996, ApJL 473, L31
Barnard E.E., 1931, Yerkes Publ. 6, 44
Bolte M., Hesser J.E., Stetson B.P., 1993, ApJL 408, L89
Brown T.M., Fergusson H.C., Davidsen A.F., Dorman B., 1997, ApJ 482, 685
Buonanno R., Buscema G., Corsi C.E., Ferraro I., Iannicola G., 1983, A&A 126, 278
Buonanno R., Corsi C.E., Buzzoni A. et al., 1994, A&A 290, 69
Buonanno R., Corsi C.E., De Biase G.A., Ferraro I., 1979, In: Sedmak G., Capaccioli M., Allen R.J. (eds)Image Processing in Astronomy, Trieste, p.354
Burgarella D., Paresce F., Quilichini V. 1995, A&A 301, 675
Carney B.W., 1976, PASP 88, 334
Cristiani S., Vio R., 1990, A&A 227, 385
Cool A.M., Grindlay J.E., Cohn H.N., Lugger P.M., Slavin S.D., 1995, ApJ 439, 695
Djorgovski S., Piotto G., Phinney E. S., Chernoff D. F., 1991, ApJL 372, L41
Dorman B., Rood R.T., O'Connell R.W., 1993, ApJ 419, 596
Downes R.A., 1986, ApJS 61, 569
Ferraro F.R., Fusi Pecci F., Cacciari C. et al., 1993, AJ 106, 2324
Ferraro F.R., Paltrinieri B., Fusi Pecci F. et al., 1997a, A&A 324, 915
Ferraro F.R. et al. , 1997b, *in preparation*
Ferraro F.R., Paltrinieri B., Fusi Pecci F. et al., 1997c, ApJ 484, L145.
Ferraro F.R., Paltrinieri B., Fusi Pecci F., Rood R.T., Dorman B., 1997d, MNRAS 292, L45
Ferraro F.R., Carretta E., Corsi C.E. et al., 1997e, A&A 320, 757
Fusi Pecci F., Ferraro F.R., Bellazani M. et al., 1993, AJ 105, 1145
Gilliland R.L, Edmonds P.D., Petro L., Shas A., Shara M., 1995, ApJ 447, 191
Green P.F., Schmidt M., Liebert J., 1986, ApJS 61, 305
Grindlay J.E., 1992, In: van den Heuvel E.P.J, Rappaport S.A. (eds) X-ray Binaries and Recycled Pulsars, NATO series 377, p. 365
Guhathakurta P., Yanny B., Bahcall J.N., Schneider D.P., 1994, AJ 108, 1786
Gunn J.E, Griffin R.F., 1979, AJ 84, 752
Harris H.C., Guetter H.H., Pier J.R. et al., 1992, AJ 104, 53
Holtzmann J.A., Burrows C.J., Casertano S. et al., 1995, PASP 107, 1065
Hut P., McMillan S., Goodman J. et al., 1992, PASP 104, 981
Irwin M.J., Trimble V., 1984, AJ 89, 83
Klemola A.R., 1979, PASP 91, 27
Kulkarni S.R. Gross W.M., Wolszczan A., Middleditch J., 1990, ApJL 363, L5
Kurucz R.L., 1992, In: B. Barbury B., & A. Renzini A. (eds) IAU Symp. 149, The Stellar Populations of Galaxies, p 225
Lyne A.G. 1995, In: Fruchter A.S., Tavani M., Backer D.C. (eds), Millisecond Pulsars- A Decade of Surprise, ASP conf. ser. Vol. 72, p 35
McLean B.J., Viner M.R., Hughes V.A., 1983, A&A 128, 434
Paltrinieri B., Ferraro F.R., Fusi Pecci F., Carretta E., 1998, MNRAS in press
Parmar A.N., 1992, In: van den Heuvel E.P.J., Rappaport S.A. (eds), X-ray Binaries and Recycled Pulsars, NATO series 377, p. 5
Roeser S., Bastian U., 1988, A&AS 74, 449
Sandage A.R., 1953, AJ 58, 61
Sawyer Hogg H., 1973, Publ. David Dunlap Obs., No 6
Shara M.M., Moffat A.F., Hanes D.A., 1985, in Dynamics of Star Clusters, Symp. IAU 113, eds J. Goodman and P. Hut, p 103
Shara M.M., Drissen L., Bergeron L. E., Paresce F. 1995, ApJ 441, 617
Webbink R.F., 1985, In: Goodman J., Hut P. (eds) Dynamics of Star Clusters Symp. IAU 113, p 541
Warner B., 1987, MNRAS 227, 23
von Zeipel F.H., 1908, Ann. Obs. Paris 25, F1

This article was processed by the author using Springer-Verlag LaTeX A&A style file *L-AA* version 3.